Laser induced fluorescence and FT-Raman spectroscopy for characterization of patinas on stone substrates

M. Oujja[1*], C. Vázquez-Calvo[2], M. Sanz[1], M. Álvarez de Buergo[2], R. Fort[2] and M. Castillejo[1]

[1]Instituto de Química Física Rocasolano, CSIC, C/ Serrano 119, 28006 Madrid, Spain

[2]Instituto de Geociencias, CSIC-UCM, C/ José Antonio Nováis 2, 28040 Madrid, Spain

[*]e-mail: m.oujja@iqfr.csic.es
Phone: 34-91-5619400
Fax: 34 915642431

Abstract This article reports on a compositional investigation of stone patinas, thin coloured layers applied for protective and/or aesthetic purposes on architectural or sculptural substrates of cultural heritage. Analysis and classification of patinas provide important information of historic and artistic interest, as their composition reflects the local practice, the availability of different materials and the building technological knowledge at specific historical periods. Model patinas fabricated according to traditional procedures and applied on limestone, and a historic patina sample from the main façade of the *San Blas* Monastery in Lerma, a village from the province of Burgos, Spain, were analyzed by laser induced fluorescence and Fourier transform-Raman spectroscopy. The results gathered demonstrate the capability of these two analytical techniques to identify the key components of each formulation and of the ensuing reaction products, which result from chemical and mineralogical transformations in the course of time, and to provide information leading to the classification of different types of patinas.

Keywords Laser induced fluorescence · FT-Raman spectroscopy · patinas · stone substrates

Introduction

Patina is a term with several meanings [1-3]. In this case it is referred to the surface treatments often found on stone substrates of cultural heritage, consisting in a thin layer applied for protective purposes and/or for modifying or unifying the colour appearance of the stone surface. When speaking of patinas it is useful to distinguish between historic patinas based on calcium oxalate and calcium phosphate (mainly studied and found in Italy, Greece and Spain) from other kind of treatments, sometimes also called patinas, such as plasters, lime putties, etc. The main components of historic patinas together with calcium oxalate and phosphate, are calcite, iron oxides or hydroxides and clay minerals, as referred by different authors [1, 2, 4, 5]. Some organic materials such as oil, egg, milk, etc., were also traditionally employed in the preparation of calcium oxalate- and calcium phosphate-based patinas [1, 3], although the mineralogical changes undergone with ageing complicate the identification of the original components. In particular regarding calcium oxalate, various mechanisms have been proposed to explain its formation from oxalic acid [6] involving weathering processes and biological activity. In turn the presence of phosphates has been related with used components, deposit of atmospheric particulates, residues of past conservation treatments and mineralization of organic protective treatments containing dairy products such as milk [4, 6, 10]. However the mentioned materials are not exclusive of patinas. One example is the case of calcium oxalate found in stone monuments which results from the reaction of calcite with ammonium oxalate, a compound used in restoration as a common stone consolidation practice [7].

Analysis and classification of patinas or other kind of treatments on stone monuments provide important information of historic and artistic interest; therefore restoration works undertaken on artistic stone façades aim at ensuring their preservation [8]. The composition of patinas and other surface treatments reflects the local practice and availability of the different materials used in their preparation. Appropriate mineralogical and chemical analysis and suitable technological knowledge serve to infer the original composition of patinas, to identify the ingredients and substances used in their preparation and the ensuing chemical and mineralogical transformations. Techniques such as X-ray diffraction, optical and fluorescence microscopies, scanning electron microscopy with energy dispersive X-ray spectrometry and electron microprobe analyzers have been used in past studies for the characterization of patina layers and have provided useful information on their composition, texture and structure [2, 9, 10]. Other spectroscopic techniques such as Fourier-transform infrared spectroscopy and gas chromatography-mass spectrometry (GC-MS) have been used to investigate the origin of oxalate films and to characterize the presence of organic materials on marble patinas [6].

Laser based spectroscopic techniques constitute an advantageous approach for the study of patinas, based on their non-invasive character and the possibility of performing in situ measurements with portable systems. Vazquez-Calvo et al. [11] have analyzed historic patinas on Spanish buildings from the 16th and 17th centuries by means of laser induced breakdown spectroscopy (LIBS), showing that this technique can assist in fast and easy characterization and classification. Other non-destructive laser spectroscopies such as laser induced fluorescence (LIF) and Raman are widely used in the analysis of cultural heritage substrates. LIF is a sensitive technique, shown in several cases to be useful for identifying differences in organic and inorganic substrates on the basis of their characteristic molecular emission bands [12-18]. Svanberg et al. [19] have used a portable LIF system to detect surface treatments

and biodeterioration layers on the stone façades of historical buildings. Due to the difficulties associated to the full identification of materials by LIF, this technique is often used in combination with other spectroscopies such as Raman, as the later can provide highly specific information on molecular composition that is complementary to the data obtained by LIF [13-15, 18]. In particular, Fourier-transform Raman spectroscopy (FT-Raman) overcomes the difficulties associated with the sometimes intense background fluorescence that accompanies the Raman signal [20]. Together with the advantages of complementary analyses using multianalytical approaches, other authors have also stressed the need of statistical methods for data treatment, in order to optimize and quantify the gathered information [21].

In this work LIF and FT-Raman spectroscopies have served to analyze model patinas of different composition. These patinas have been fabricated according to traditional procedures using recipes obtained through a recent study on historical surface treatments of Spanish stone heritage and which reflect the availability of local products [3]. The patinas studied herein were selected from a total of 33 different combinations of various components prepared in the framework of a broader study aiming at the identification of mixtures used for obtaining artificial oxalate- and phosphate-based treatments [22]. For this work, two set of model patinas, out of a total of five samples, with milk and oxalic acid as main components, were analyzed. Oxalic acid was chosen in this study because this compound is considered to be the origin of calcium oxalate films in patinas, either involving metabolic biological activity or through chemical processes [6]. A historic oxalate and phosphate patina, sampled from the main façade of the *San Blas* Monastery in Lerma, a village from the province of Burgos, Spain, and previously characterized by other techniques [2], was also analyzed.

Although the investigation presented was carried out with laboratory LIF and FT-Raman equipment, the choice of these two non-invasive techniques was motivated by the possibility of performing measurements in situ with portable systems. The information gathered by combining the results provided by these two laser-based analytical techniques allows the identification of the main components of each formulation and of the ensuing reaction products that result from chemical and mineralogical transformations in the course of time.

Experimental

The model samples used for this investigation consist on limestone substrates on which a mixture of components was applied in order to produce a coating of around 400 µm thickness, covering a surface of 3x5 cm^2 (Fig. 1). Limestone is a sedimentary rock largely composed of calcite ($CaCO_3$); here, blocks of the *Páramo geological formation* (Upper Miocene, Madrid Basin), specifically from "*Colmenar de Oreja*" variety, were used [23]. The mixture of components was applied on the stone surface by brushing. Table 1 lists the materials used for their preparation and the weight percent of each component. The samples were naturally aged for a period of one year under open air conditions prior to the present experiments. Another set of samples was also prepared by applying on limestone blocks a coating of each of the individual components used in the formulation of the patinas. These components are lime paste (calcium hydroxide, $Ca(OH)_2$, provided by Emilio Quilez, Spain), unpasteurized goat milk, linseed oil (CTS, Spain), ochre pigment (iron oxyhydroxide, FeO(OH), CTS, Spain) mixed with water and oxalic

acid 2-hydrate ($(COOH)_2.2\ H_2O$, Panreac, Spain) also mixed with water. Besides, a sample of a historic patina from the main façade of *San Blas* Monastery (Baroque style, 17th cc, Lerma, Burgos, Spain), previously characterized by XRD and microscopic techniques [2], was analyzed by means of laser induced fluorescence (LIF) and Fourier transform-Raman spectroscopy (FT-Raman) together with the model samples.

LIF was excited at 266 nm using the unfocused output of the fourth harmonic of a Q-switched Nd:YAG laser (Quantel, Brilliant B, pulse width 5 ns, repetition rate 10 Hz) [12]. The beam illuminated the surface of the sample at 45º with a beam spot diameter of 1 mm and energy per pulse of around 0.1 mJ. The emitted fluorescence was collected at right angles with respect to the incident laser and imaged with a lens onto the entrance slit of a 0.30 m spectrograph (TMc300 Bentham, 300 grooves/mm, 500 nm blaze). The spectrograph was coupled to a time gated ICCD camera (2151 Andor Technologies) that was placed at its exit slit. The spectra were recorded, in intervals of 300 nm, in the 300-650 nm wavelength range, with a resolution of 5 nm. The light emitted upon irradiation with each laser pulse was collected within a temporal gate of 3 µs, at zero delay with respect to the arrival of the laser pulse to the sample surface. For the results presented here, a 300 nm cutoff filter was set in front of the spectrograph to avoid the second order emissions of lower wavelengths.

FT-Raman spectra were recorded on a Bruker MultiRAM spectrometer (Bruker Optics) with a liquid-nitrogen cooled Ge diode as detector. A cw-Nd:YAG-laser at 1064 nm was used as excitation source of Raman scattering. The spectra were recorded with a laser power output of 60 mW over the range of 3500-100 cm^{-1} with a spectral resolution of 4 cm^{-1}. The light scattered from an area < 0.01 cm^2 of the sample was collected in backscattering (or 180°) geometry. Double analysis with a total scan number of 200 was executed for each sample. The peak heights of the resulting average spectra were obtained after vector-normalization using the operating software OPUS Ver. 6.5 (Bruker Optics).

Results and discussion

Laser induced fluorescence spectra of model patinas

LIF spectra were collected on the bare limestone surface, on each of the five different patina components and on the five prepared model patinas (Table 1). These are shown in Figs. 2 and 3. Before discussing the assignment of the LIF spectral features it should be indicated that the peak at 532 nm observed in Figure 2b,c and Figure 3b,c is due to residual second harmonic of the Nd:YAG laser used to excite the fluorescence.

Figure 2a shows the spectra of the bare limestone surface which consist in two broad bands centred at 350 and 500 nm. These emissions are assigned, in agreement with reported studies [24, 25], to acid-extractable organics and bitumen, usually present in the stone as an organic carbon fraction [25] and which are the main limestone fluorophores. It is important to note that the contribution to the measured LIF spectra of the underlying limestone should be negligible due to the strong UV absorption of the

individual patinas components and to the large thickness of the patina layers. The LIF spectrum of lime paste (Fig. 2b) consist on a broad band ranging from 300 to 650 nm with some overimposed structure with local maxima at 370, 400 and 430 nm [26]. These fluorescent emissions can be assigned to the organic residues of lime paste, fabricated, according to the manufacturer (see Experimental section), by mixing calcinated limestone, water and some animal fat. As shown below, the presence of peaks of organic origin in the FT-Raman spectra of this material support such assignment.

Spectra recorded on goat milk coated limestone (Fig. 2c) present two characteristic bands centered at 350 and 430 nm with shoulders around 395, 480 and 520 nm. The main fluorophores in milk are aromatic amino acids and nucleic acids, lipids, vitamin A and riboflavin. The three protein amino acids that contribute to UV fluorescence are tyrosine (2.8 %), phenylalanine (3.9 %) and tryptophan (1.2 %) [15]. In neutral aqueous solution, the quantum yields of tyrosine and tryptophan are 0.14 and 0.20 respectively [27] while the quantum yield of phenylalanine is small, typically about 0.03, so the emission from this residue is rarely observed. Upon excitation at 266 nm tyrosine and tryptophan have a maximum emission at 315 and 350 nm respectively [15]. On the other hand products of oxidation, combination and modification of amino acids, such as dityrosine, 3,4-dihydroxyphenylalanine (DOPA), N-formylkynurenine (NFK) and kynurenine display emissions in the 400–500 nm region [16, 28], while phospholipids give rise to fluorescence emissions in the 520–570 range [28]. According with this information the fluorescence recorded in the goat milk coated limestone centered at 350 nm is assigned to tryptophan while the longer broad wavelength band is ascribed to degradation and oxidation products (dityrosine, DOPA, NFK and kynurenine) and phospholipids are mainly responsible for the shoulder observed at 520 nm. Riboflavin and other crosslinking products, resulting of the reaction between amino acids and sugar or lipids of milk, also contribute to the observed wide emission [17].

The LIF spectrum of the linseed oil applied on limestone is presented in Fig. 2d. As reported in the literature, a broad band in the 400- 600 nm region is a distinctive feature of this oil [29]. While LIF emission of the ochre pigment coating (not shown) is characteristically weak [30], the spectrum of oxalic acid 2-hydrate (Fig. 2e) consists on a strong band extending from 300 to 450 nm. This band is due to the $\pi^* \rightarrow n$ transition emission from free oxalic acid [31]. The observed peaks around 340 and 355 nm are due to hydroxyl radicals [12].

Figure 3 displays the LIF spectra of the model patinas. Shown in Fig. 3a is the spectrum of patina S1 resulting from the mixture of lime paste and goat milk. The overall fluorescence intensity is higher than that of the individual components (Figs. 2b, c) and the relative increase of the 460 nm feature, with respect to the shorter wavelength band at around 350 nm, is explained by the presence of milk oxidation products resulted from the oxidative effect of lime paste over the constituent milk proteins which emissions are predominant in this region. LIF spectra of patinas S2 and S3 (Fig. 3a) display a similar appearance and show a more intense short wavelength band in the region of 350 nm as compared with the spectrum of patina S1. This effect is related with the presence of linseed oil in S2 and linseed oil and ochre in S3 which restrict the oxidation effect induced by lime paste on the milk proteins. Figure 3a indicates that the addition of linseed oil to the composition of patina S1 does not induce any changes in the fluorescence between 450-650 nm.

The fluorescence bands characterizing the patinas S4 and S5 consist on a broad fluorescence emission ranging from 300 to 650 nm (Fig. 3b). This emission differs from that of lime paste (also displayed, as taken from Fig. 2b, for comparison) by a somewhat higher intensity and a slight widening in the 450-600 nm spectral region. This difference is ascribed to the presence of calcium oxalate compounds formed by coordination of the free $C_2O_4^{2-}$ ligands of oxalic acid to the calcium hydroxide of lime paste [31]. Addition of ochre, a pigment of negligible fluorescence, to yield the formulation of patina S5, does not introduce any spectral modification.

Figure 3c shows a comparison between LIF spectra of patina S1, lime paste and goat milk. The emission in the region between 450-550 nm is attributed to fluorophores different from those present in the composition of lime paste and of goat milk. Hence, the emission in this region is assigned to products of oxidation and combination of amino acids of goat milk induced by the effect of lime paste.

FT-Raman spectra of model patinas

FT-Raman spectra of each of the different patina components, and of the five model patinas are shown in Figures 4 and 5 respectively. Table 2 lists the bands observed with the corresponding assignments.

The spectrum of limestone (Fig. 4) displays characteristic bands of calcium carbonate, which correspond to the vibration modes of the free CO_3^{2-} ion. These bands are attributed to lattice vibrations, to in-plane bending and symmetric stretch modes. Bands of organic residues assigned to δ_a (C-H) of methylene groups (α-CH_3 and O-CH_3), of lipids and amino acids and to ν(C=O) stretching of fatty acid esters [33] are also observed. Lime paste, mostly composed of portlandite (calcium hydroxide), quickly transforms into calcite, which explains the presence of the above bands. In addition to the calcium carbonate bands, the FT-Raman spectrum of lime paste displays also bands assigned to organic residues and to hydrated lime ($Ca(OH)_2$) [32]. It could be argued that these bands are produced by the underlying limestone substrate; however as mentioned before, the lime paste layer is thick enough, over 400 µm, to avoid the Raman excitation of the limestone material. The FT-Raman spectrum of goat milk on limestone substrate (Fig.4) shows bands assigned to tryptophan, to amide III of the proteins backbone, to in phase methylene twist and to ν(CC) aromatic ring chain vibrations. The bands observed in the region of 2750-3100 cm^{-1} are attributed to the ν(C–H) mode of the aliphatic compounds present in milk [17, 18]. Bands of calcite are also observed in the FT-Raman spectrum of goat milk and are due to the limestone substrate. FT-Raman spectrum of linseed oil on limestone is similar to the corresponding to limestone with an additional band at 1302 cm^{-1} corresponding to the in phase methylene twist. Finally, the FT-Raman spectrum of oxalic acid shows bands corresponding to this compound [34] and the calcite band at 1085 cm^{-1} due to the limestone substrate.

FT-Raman spectra of the five model patinas are presented in Fig. 5. They are grouped in two sets with similar appearance. Spectra of patinas containing milk (S1-S3) appear in Fig. 5a and those based on oxalic acid (S4, S5) in Fig. 5b. A common set of bands at 154, 281, 711, 780, 1085, 1445 and 1744 cm^{-1} are observed in all five spectra. As indicated before, these bands are due to lime paste, a compound present in all studied model patina formulations.

Additionally, the spectra of patinas S1, S2 and S3 (Fig. 5a) show the presence of bands assigned to tryptophan, to amide III of the proteins backbone, to in phase methylene twist, to ν(CC) aromatic ring chain vibrations and to the ν(C–H) mode of the aliphatic compounds of milk. These bands are less intense than in the case of goat milk applied on limestone due to the oxidation of milk component under the presence of lime paste.

Figure 5b shows the FT-Raman spectra of patinas S4 and S5 based in mixtures of lime paste and oxalic acid 2-hydrate. The bands related with the lime paste component are accompanied by a set of bands. These are characteristic of calcium oxalate monohydrate ($CaC_2O_4.H_2O$, whewellite) [35, 36] which, as already mentioned in the description of the corresponding LIF spectra, it is formed by neutralization of the oxalic acid ($C_2H_2O_4$) by calcium hydroxide ($Ca(OH)_2$) of the lime paste in presence of water. Table 2 gives in detail the assignment of the oxalate bands characteristic of the monohydrate species. Finally, the presence of ochre in patina S5, Fig. 5b is noticed by an extra band at 385 cm^{-1} attributed to yellow ochre pigment used in the preparation of this patina [20].

Although we can not completely rule out some organic contamination on the model samples due to exposure to ambient air during the ageing period, spectral differences, both LIF and FT-Raman, found between the two groups, based on milk and based on oxalic acid, are representative enough to validate the study.

Analysis of historic patina

LIF and FT-Raman spectra of the historic patina sample, which displays an orange/brown like patination layer, were also recorded. These are shown in Fig. 6 and Table 3 lists the bands observed in the FT-Raman spectrum with the corresponding assignment. The LIF spectrum (Fig. 6a) consists on a broad band peaking at 350 nm and a shoulder at 470 nm. Comparison between spectra of Fig. 2 and Fig. 3b of individual patina components and oxalates based patinas respectively, suggests that the historic patina is based on oxalates rather than on proteinaceous components. More specific information on its composition is obtained via FT-Raman analysis (Fig. 6b).

FT-Raman spectrum of the substrate of historic patina (Fig. 6b) reveals the presence of a mixture of calcite and gypsum. On the other hand, the spectrum of the historic patina contains bands attributed to $CaCO_3$ as calcite, gypsum, hydroxyapatite (calcium phosphate), ivory black and calcium oxalates. The presence of gypsum is considered as a result of weathering processes and not an original component of the patina, due to its less intense bands. Although the broad band observed at 780 cm^{-1} was attributed previously in model patinas to hydrated lime ($Ca(OH)_2$, portlandite) (Fig. 4), in this case this band is due to the characteristic luminescence emission of hydroxyapatite and related minerals [37]. The presence of hydroxyapatite is related to the ivory black based on bones which contain a high concentration of phosphates (PO_4^{3-}) [20]. No iron oxides, which could be responsible of the orange/brown coloration of the patina, were detected. The FT-Raman spectrum of historic patina does not contain any band that could be directly related with proteins and lipids indicating that these organic products, if present in the patina, are

in quantities below the detection limit of the technique. Full characterization of these trace elements would require sample extraction and the use of more sensitive techniques such as GC-MS.

Conclusions

The combined application of two laser based non-invasive techniques such as laser induced fluorescence and FT-Raman spectroscopy for the study of model patinas on limestone substrates has allowed the identification of the main patina compounds and products of some of the chemical and mineralogical transformations undergone with the course of time. As shown, LIF analysis provided an initial identification of characteristic fluorophores, as is the case of emission from amino acids in the region around 350 nm. Products derived from the reaction of individual components also show their distinctive broad band emissions, i.e calcium oxalates formed by reaction of oxalic acid and calcium hydroxide. FT-Raman results supply distinctive molecular signatures of individual components and of products of chemical and mineralogical transformations, in particular of calcium oxalate monohydrate. Application of this methodology to an historic patina has allowed the identification of its components based mainly in calcite, calcium oxalates and phosphates. Although it was not possible to determine the organic content of the historic patina due to the characteristics of the sample, it was proved in the case of model patinas that these techniques are useful for examination of patinas or renderings, especially in cases where organic materials have not been completely chemically or mineralogically transformed into inorganic compounds. As portable systems are available for performing in situ LIF and FT-Raman measurements, the information obtained in the present work demonstrates that the combined application of these two spectroscopic techniques can assist the practice of conservation as regards the classification of patinas used on historic stone heritage. Work is in progress to analyze a larger number of historical patinas to validate the conclusions of this initial investigation.

.

Acknowledgements This work has been funded by Madrid Regional Government project Geomateriales (S2009/Mat-1629) and by Ministerio de Ciencia e Innovación under Projects CTQ2010-15680 and CONSOLIDER CSD2007-00058. The authors thank also the research Group from Universidad Complutense de Madrid: "*Alteración y Conservación de los Materiales Pétreos del Patrimonio*".

References

1. Álvarez de Buergo M, Fort R (2003) Constr Build Mater 17: 83
2. Vázquez-Calvo C, Álvarez de Buergo M, Fort R (2006) In: Fort R, Álvarez de Buergo M, Gómez-Heras M, Vázquez-Calvo C, (eds) Heritage Weathering and Conservation 969- 974, Taylor & Francis/ Balkema, Leiden
3. Vázquez-Calvo C, Álvarez de Buergo M, Fort R (2007) In: Prikryl R, Smith B (eds.) Building Stone Decay: from Diagnosis to Conservation, The Geological Society of London. Special Publications. 271: 295
4. Kouzeli K, Lazari C, Economopoulos A, Pavelis C (1996) in: Realini M, Toniolo L (eds.) The oxalate films in the conservation of works of arts; Proc 2nd Intern Symp 83-93, Milan, Castello d'Argile: EDITEAM s.a.s.
5. Polikreti K, Maniatis Y (2003) The Science of the Total Environment 308 (1-3): 111
6. Rampazzi L, Andreotti A, Bonaduce I, Colombini MP, Colombo C, Toniolo L (2004) Talanta 63: 967
7. Taniguchi Y, Shimadzu Y, Kakoulli I (2003) in: 25th Annual Conference of Japan Society for Conservation for Cultural Property, Kyoto Zokei University
8. Cooper M, Larson J (1996) The Conservator 20: 28
9. Vázquez-Calvo C, Gomez Tubio B, Álvarez de Buergo M, Ortega Feliu I, Fort R, Respaldiza MA (2008) X-Ray Spectrom 37: 399
10. Vázquez-Calvo C, Álvarez de Buergo M, Fort R, Varas MJ (2007) Mater Charact 58 (11-12): 1119
11. Vázquez-Calvo C, Giakoumaki A, Anglos D, Álvarez de Buergo M, Fort R (2007) In: Nimmrichter J, Kautek W, Schreiner M (eds.) Lasers in the conservation of artworks, Springer Proceedings in Physics, 116: 415-420, Springer–Verlag, Viena
12. Oujja M, García A, Romero C, Vázquez de Aldana JR, Moreno P, Castillejo M (2011) Phys Chem Chem Phys 13: 4625
13. Castillejo M, Martín M, Oujja M, Silva D, Torres R, Manousaki A, Zafiropulos V, Van den Brink OF, Heeren RMA, Teule R, Silva A, Gouveia H (2002) Anal Chem 74: 4662
14. Gaspard S, Oujja M, Moreno P, Méndez C, García A, Domingo C, Castillejo C (2008) Appl Surf Sci 255: 2675
15. Gaspard S, Oujja M, Abrusci C, Catalina F, Lazare S, Desvergne JP, Castillejo M (2008) J Photochem Photobiol A 193: 187
16. Wisniewski M, Sionkowska A, Kaczmarek H, Lazare S, Tokarev V, Belin C (2007) J Photochem Photobiol A: Chem 188: 192
17. Nevin A, Osticioli I, Anglos D, Burnstock A, Cather S, Castellucci E (2007) Anal Chem 79: 6143
18. Oujja M, Pouli P, Fotakis C, Domingo C, Castillejo M (2010) Appl Spectrosc 64: 528
19. Weibring P, Johansson T, Edner H, Svanberg S, Sundnér B, Raimondi V, Cecchi G, Pantani L (2001) Appl Opt 40: 6111
20. Bell IM, Clark RJH, Gibbs JP (1997) Spectrochim Acta Part A 53: 2159
21. Raimondi V, Cecchi G, Lognoli D, Palombi L, Grönlund R, Johansson A, Svanberg S, Barup K, Hällström J (2009) Int Biodet Biodeg 63: 823
22. Vázquez-Calvo C, Álvarez de Buergo M, Fort R (2009) WO 2009024642 (A1) - Publication date: 2009-02-26, application number: WO2008ES70165 20080813, priority number(s): ES20070002293 20070816
23. Bustillo A (1980) Boletín Geológico y Minero XCI-III: 503
24. Wang J, Wu X, Mullins C (1997) Appl Spectrosc 51: 1890
25. Bezouska JR, Wang J, Mullins OC (1998) Appl Spectrosc 52 : 1606
26. Aminzadeh A (1997) Spectrochimica Acta Part A 53: 693
27. Teale FWJ, Weber G (1957) Biochemical Journal 65: 476
28. Palumbo G, Pratesi R (2004) Lasers and Current Optical Techniques in Biology, Comprehensive Series in Photochemistry and Photobiology, Royal Society of Chemistry, Cambridge UK
29. Nevin A, Comelli D, Valentini G, Cubeddu R (2009) Anal Chem 81: 1784
30. Athanassia A, Hill AE, Fourrier T, Burgio L, Clark RJH (2000) J Cult Herit 1: S209
31. Lu J, Li Y, Zhao K, Xu JQ, Yu JH, Li GH, Zhang X, Bie HY, Wang TG (2004) Inorg Chem Commun 7: 1154
32. Taddei P, Tinti A, Gandolfi MG, Rossi PL, Prati C (2009) J Mol Struct 924-926 : 548
33. Nevin A, Comelli D, Osticioli I, Filippidis G, Melessanaki K, Valentini G, Cubeddu R, Fotakis C (2010) Appl Phys A 100: 599
34. Jeziorowski H, Moser B (1985) Chem Phys Lett 120: 41
35. Frost RL (2004) Analytica Chimica Acta 517: 207

36. Shippey TA (1980) J Mol Struct 63: 157
37. Campos-Suñol MJ, Domínguez-Vidal A, Ayora-Cañada MJ, De la Torre-López MJ (2008) Anal Bioanal Chem 391:1039

Table 1 Composition of model patinas applied on limestone substrates with weight percent of each component between brackets

S1	Lime paste (54%), unpasteurized goat milk (46%)
S2	Lime paste (50%), unpasteurized goat milk (43%), linseed oil (7%)
S3	Lime paste (50%), unpasteurized goat milk (43%), linseed oil (7%), ochre (1%)
S4	Lime paste (28%), oxalic acid 2-hydrate (36%), distilled water (36%)
S5	Lime paste (28%), oxalic acid 2-hydrate (36%), distilled water (36%), ochre (2%)

Table 2 Assignments of bands in the FT-Raman spectra of model patinas and of their individual components. The first column marks between parentheses the patinas containing the corresponding band

Wavenumbers (cm^{-1})	Vibrational assignment	Origin of bands
2750-3100 (S1-S3)	ν(C-H) of aliphatic compounds	Milk
1744 (S1-S5)	ν(C=O) stretching of fatty acid esters	Organic residues, milk, linseed oil
1728 (S4, S5)	ν_a(C=O) of oxalate	Whewellite
1656 (S1-S3)	δ(N-H), amide I	Milk proteins
1630 (S4, S5)	ν_a(C-O) of oxalate	Whewellite
1580-1600 (S1-S3)	ν(CC) aromatic ring chain vibrations	Milk
1495	δ(C-O-O) of $C_2O_4^{2-}$	Oxalic acid 2-hydrate
1491 (S4, S5)	ν(C-O) stretching, oxalate	Whewellite
1463 (S4, S5)	ν(C-O) stretching, oxalate	Whewellite
1445 (S1-S5)	δ_a(C-H) of α-CH_3 and of O-CH_3, lipids, amino acids	Organic residues, milk, linseed oil
1397 (S4, S5)	ν_s(C-O) + ν (C-C) of oxalate	Whewellite
1302 (S1-S3)	in phase methylene twist	Organic residues, milk, linseed oil
1240 (S1-S3)	δ(N-H), amide III	Milk
1085 (S1-S5)	Symmetric stretching of CO_3^{2-}	$CaCO_3$ in lime paste and limestone
939 (S4, S5)	Water libration of oxalate	Whewellite
895 (S4, S5)	ν(C-C) of oxalate	Whewellite
873 (S2, S3)	Tryptophan	Milk proteins
864 (S4, S5)	ν(C-C) of oxalate	Whewellite
857	δ(C-C-O) of $C_2O_4^{2-}$	Oxalic acid 2-hydrate
780 (S1-S5)	$Ca(OH)_2$	Hydrated lime in lime paste
711 (S1-S5)	In-plane bending of CO_3^{2-}	$CaCO_3$ in lime paste and limestone
592 (S4, S5)	ρ_s(O-C-O) of oxalate	Whewellite
560	ν(C-C) stretching, $C_2O_4^{2-}$	Oxalic acid 2-hydrate
517 (S4, S5)	δ_s(O-C-O) of oxalate	Whewellite
499 (S4, S5)	δ(O-C-O) of oxalate	Whewellite
482	δ(C-C-O) of $C_2O_4^{2-}$	Oxalic acid 2-hydrate
385 (S5)	Yellow ochre	Yellow ochre pigment
360	$Ca(OH)_2$	Hydrated lime in lime paste
281 (S1-S5)	Lattice vibration of CO_3^{2-}	$CaCO_3$ in lime paste and limestone
224 (S4, S5)	Water libration of oxalate	Whewellite
209 (S4, S5)	T_1Ca^{2+} of oxalate	Whewellite
194 (S4, S5)	T_2Ca^{2+} of oxalate	Whewellite
154 (S1-S5)	Lattice vibration of CO_3^{2-}	$CaCO_3$ in lime paste and limestone
141 (S4, S5)	τ(C-C) of oxalate	Whewellite

Table 3 Assignments of bands in the FT-Raman spectra of historic patina and its substrate from the façade of *San Blas* Monastery, Lerma, Burgos, Spain

Wavenumbers (cm^{-1})	Vibrational assignment	Origin of bands
1580	Carbon	Ivory black
1490	ν(C-O) stretching of $C_2O_4^{2-}$	Calcium oxalate
1464	ν(C-O) stretching of $C_2O_4^{2-}$	Calcium oxalate
1325	Carbon	Ivory black
1132	ν_3(S-O) mode of SO_4^{2-}	Gypsum
1085	Symmetric stretching of CO_3^{2-}	$CaCO_3$
1007	ν_1(S-O) mode of SO_4^{2-}	Gypsum
961	ν_1 (a_1) symmetric streching of PO_4^{3-}	Ivory black
780	Luminescence emission	Hydroxyapatite
711	In-plane bending of CO_3^{2-}	$CaCO_3$
670	ν_4(S-O) mode of SO_4^{2-}	Gypsum
619	ν_4(S-O) mode of SO_4^{2-}	Gypsum
493	ν_2(S-O) mode of SO_4^{2-}	Gypsum
414	ν_2(S-O) mode of SO_4^{2-}	Gypsum
281	Lattice vibration of CO_3^{2-}	$CaCO_3$
181	ν_1(S-O) mode of SO_4^{2-}	Gypsum
154	Lattice vibration of CO_3^{2-}	$CaCO_3$

Figure captions

Fig. 1 Model patina sample S4, a) and cross section observed under microscope (the dashed line shows the contact between the model patina layer (top) and the stony substrate (bottom)), b) of the patina layer on a limestone substrate

Fig. 2 LIF spectra upon excitation at 266 nm of limestone, a) and of individual patina components applied on limestone: lime paste, b); goat milk, c); linseed oil, d); and oxalic acid 2-hydrate, e). Spectral resolution is 5 nm

Fig. 3 LIF spectra upon excitation at 266 nm of model patinas: S1, S2 and S3, a); lime paste, S4 and S5, b); lime paste, goat milk and patina S1 c). Spectral resolution is 5 nm

Fig. 4 FT-Raman spectra of limestone and of individual patina components applied on limestone: lime paste, goat milk, linseed oil, and oxalic acid 2-hydrate

Fig. 5 FT-Raman spectra of model patinas S1, S2 and S3, a); and of model patinas S4 and S5, b)

Fig. 6 LIF, a) and FT-Raman spectra, b) of historic patina sample from the façade of *San Blas* Monastery, Lerma, Burgos, Spain. In a) spectra of lime paste and oxalic acid 2-hydrate and in b) the Raman spectrum of the stone substrate are shown for comparison

Fig. 1

a)

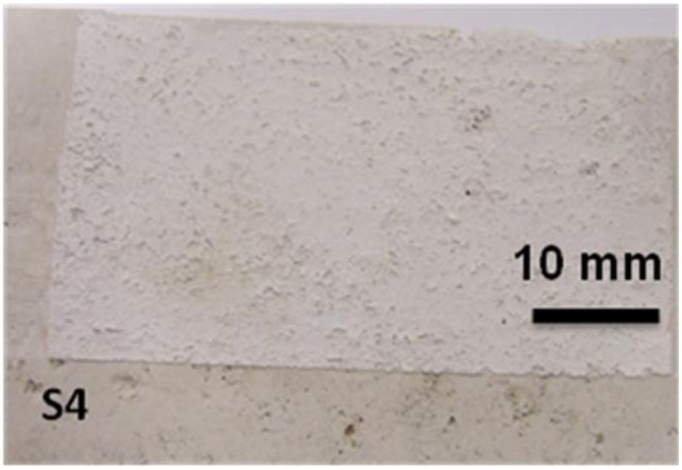

b)

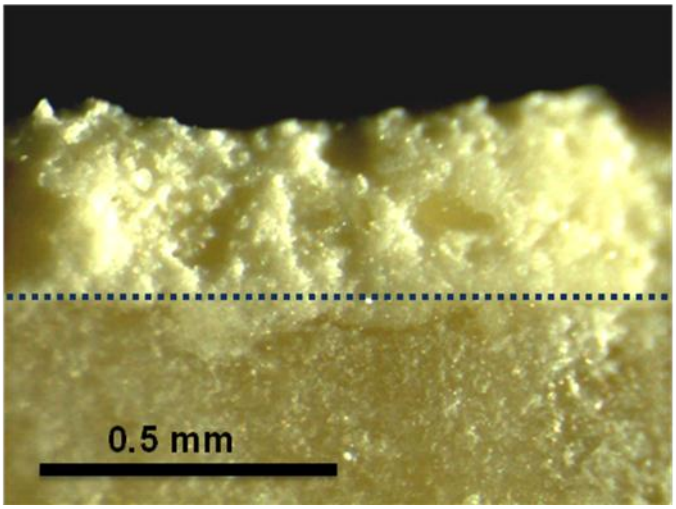

Fig. 2

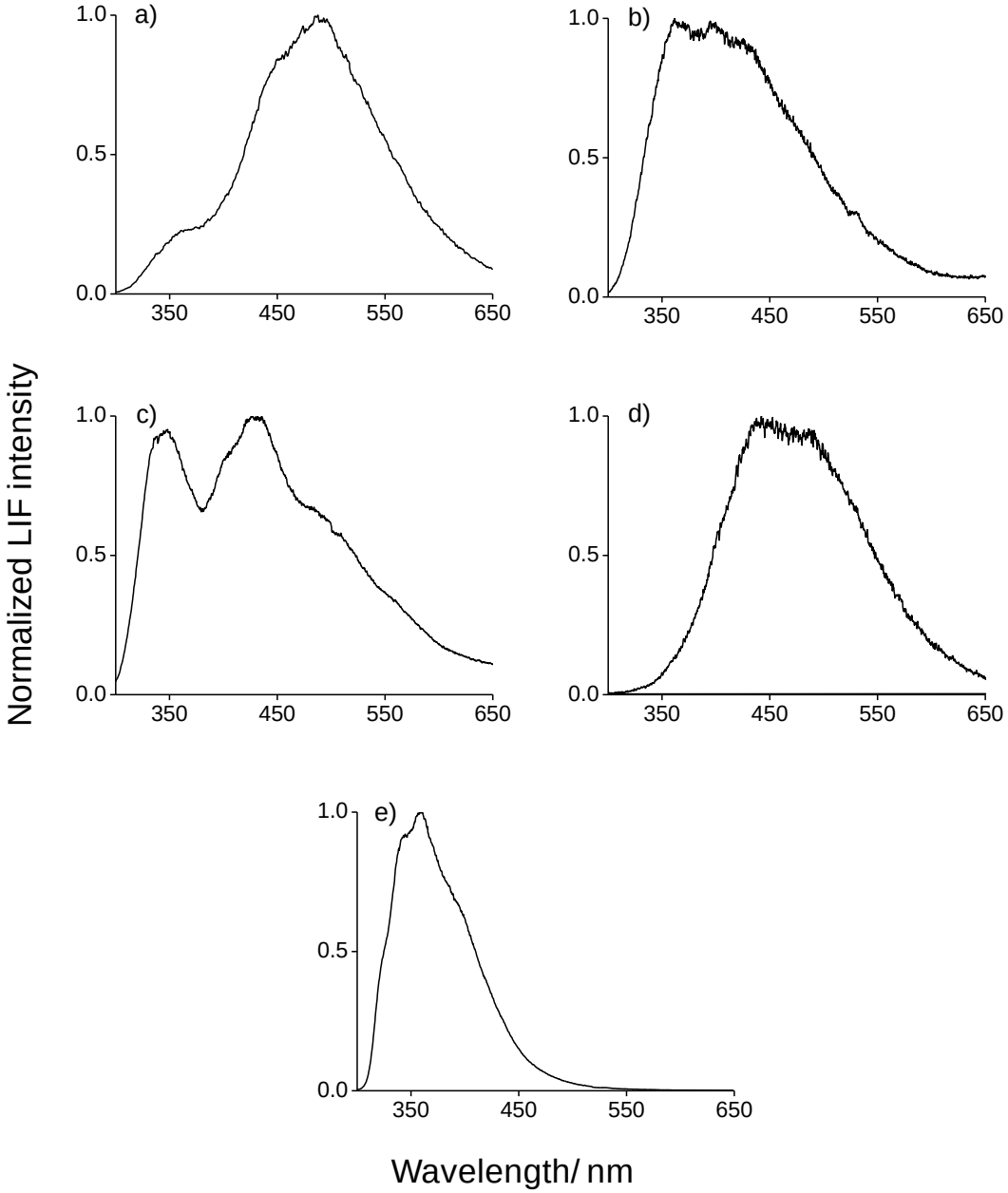
a)
b)
c)
d)
e)
1.0
0.5
0.0
350
450
550
650
Normalized LIF intensity
Wavelength/ nm

Fig. 3

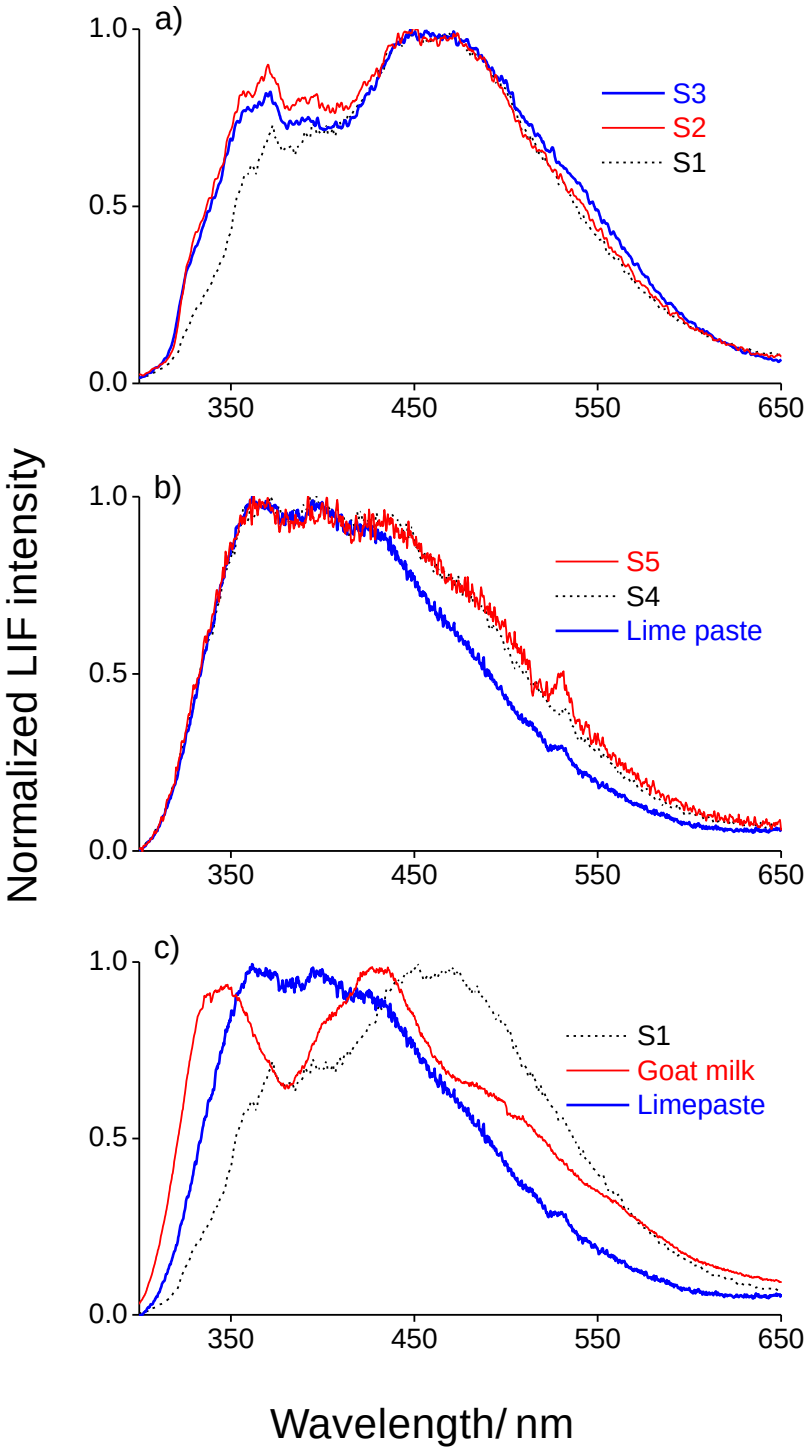
a)
1.0
0.5
0.0
350
450
550
650
S3
S2
S1
b)
S5
S4
Lime paste
c)
S1
Goat milk
Limepaste
Normalized LIF intensity
Wavelength/ nm

Fig.4

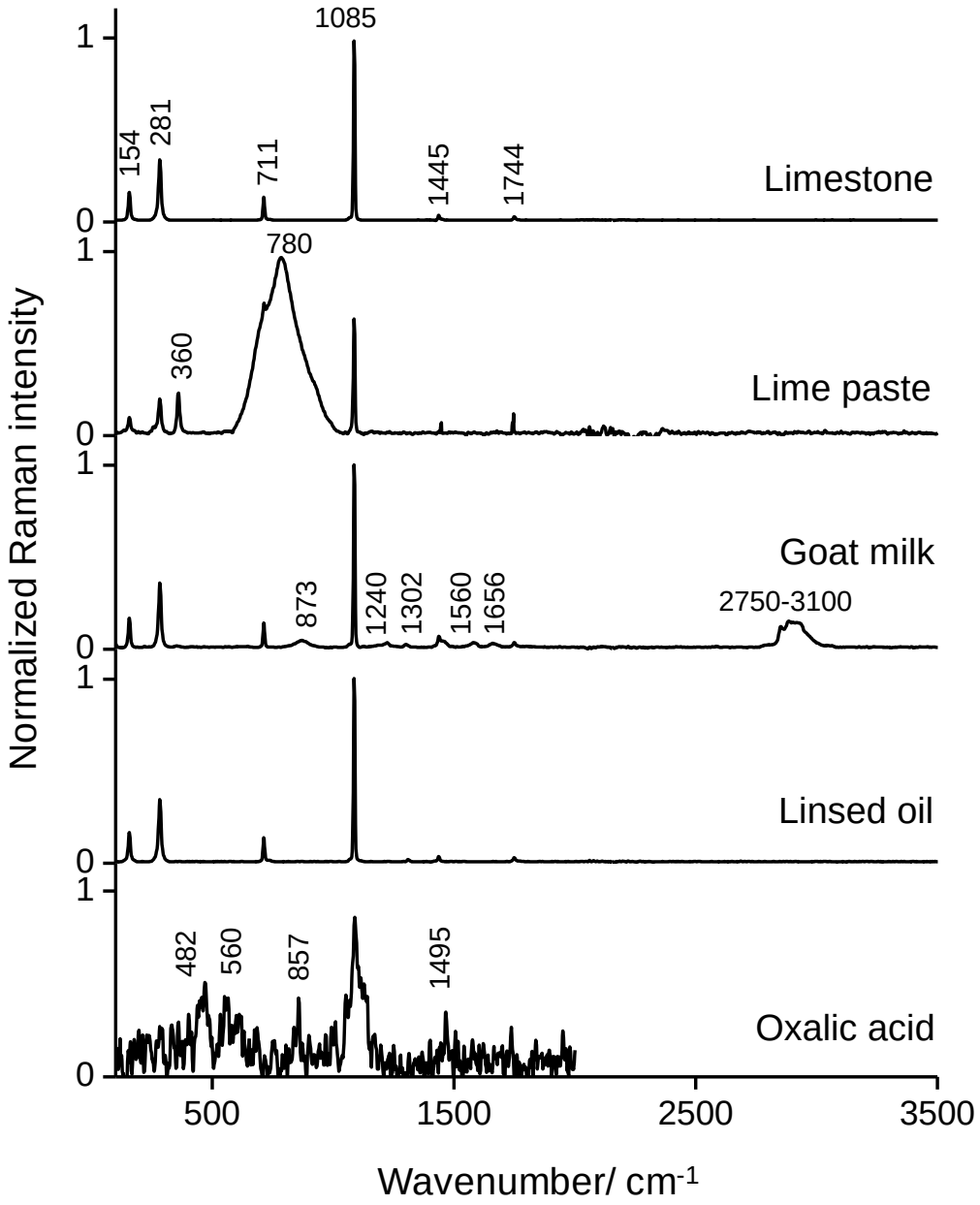
Normalized Raman intensity
Wavenumber/ cm-1
Limestone
Lime paste
Goat milk
Linsed oil
Oxalic acid
1085
154
281
711
1445
1744
780
360
873
1240
1302
1560
1656
2750-3100
482
560
857
1495
0
1
500
1500
2500
3500

Fig. 5

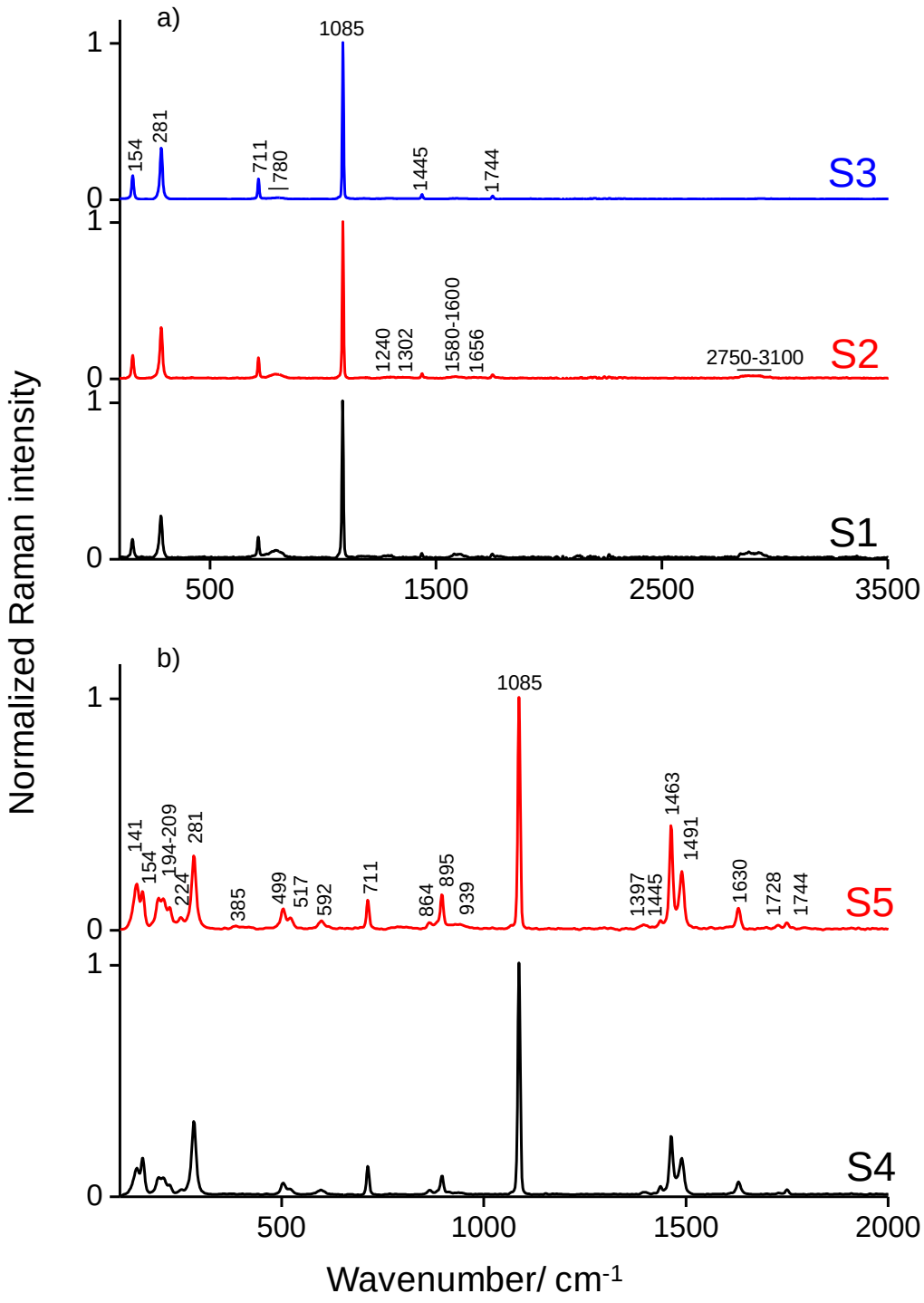
a)
1085
154
281
711
780
1445
1744
S3
1240
1302
1580-1600
1656
2750-3100
S2
S1
500
1500
2500
3500
b)
1085
141
154
194-209
224
281
385
499
517
592
711
864
895
939
1397
1445
1463
1491
1630
1728
1744
S5
S4
500
1000
1500
2000
Normalized Raman intensity
Wavenumber/ cm-1

Fig. 6

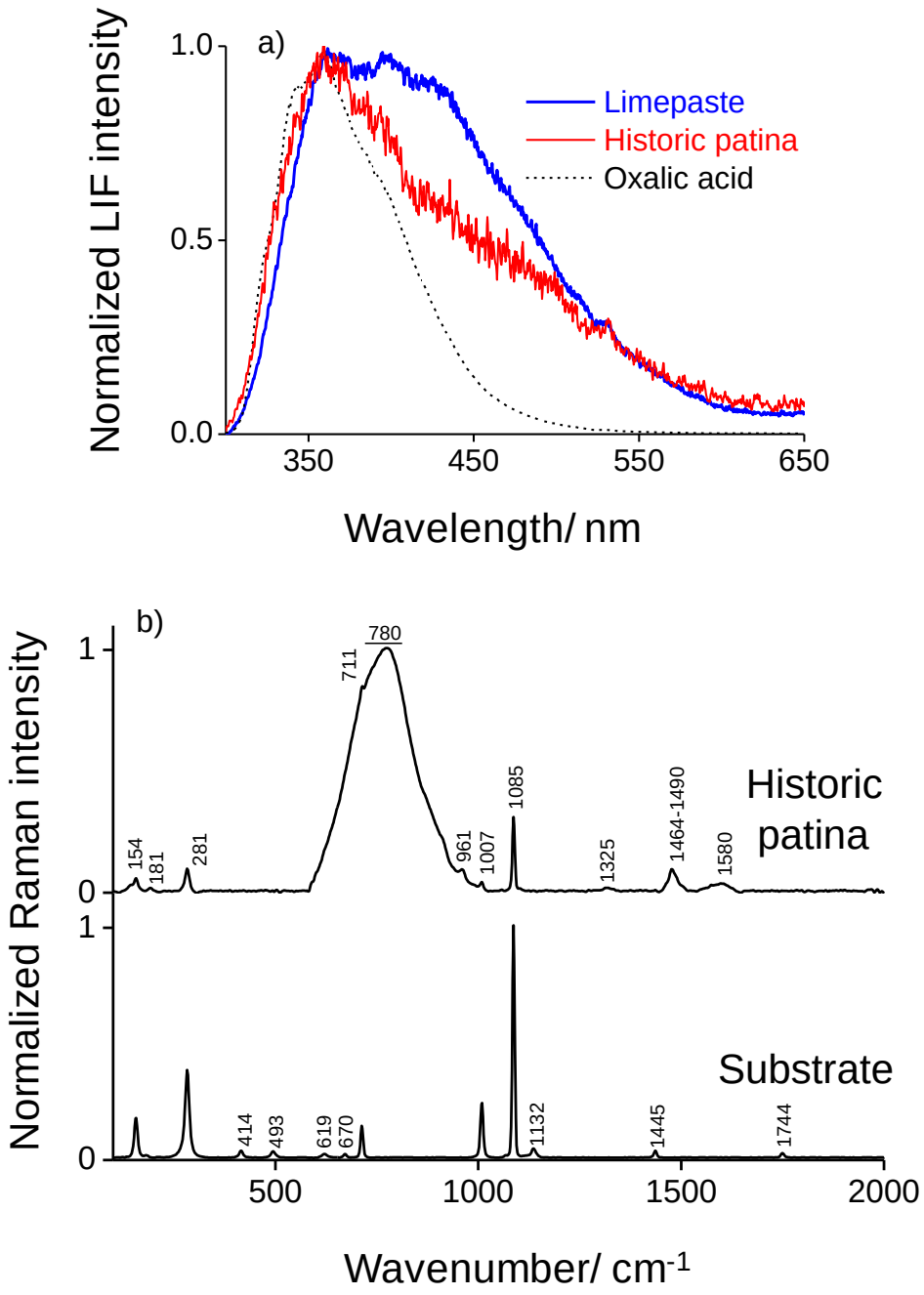
a)
Normalized LIF intensity
1.0
0.5
0.0
350
450
550
650
Wavelength/ nm
Limepaste
Historic patina
Oxalic acid
b)
Normalized Raman intensity
1
0
780
711
154
181
281
961
1007
1085
1325
1464-1490
1580
Historic patina
414
493
619
670
1132
1445
1744
Substrate
500
1000
1500
2000
Wavenumber/ cm-1